Tilt Aftereffect and Adaptation-Induced Changes in Orientation Tuning in Visual Cortex

Dezhe Z. Jin, Valentin Dragoi, Mriganka Sur and H. Sebastian Seung

JN 94:4038-4050, 2005. First published Aug 31, 2005; doi:10.1152/jn.00571.2004

Journal of Neurophysiology publishes original articles on the function of the nervous system. It is published 12 times a year (monthly) by the American Physiological Society, 9650 Rockville Pike, Bethesda MD 20814-3991. ISSN: 0022-3077, ESSN: 1522-1598. Visit our website at http://www.the-aps.org/.

J Neurophysiol 94: 4038–4050, 2005.
First published August 31, 2005; doi:10.1152/jn.00571.2004.

Tilt Aftereffect and Adaptation-Induced Changes in Orientation Tuning in Visual Cortex

Dezhe Z. Jin,[1] Valentin Dragoi,[2] Mriganka Sur,[3] and H. Sebastian Seung[4]

[1]*Department of Physics, Pennsylvania State University, University Park, Pennsylvania;* [2]*Department of Neurobiology and Anatomy, University of Texas Medical School at Houston, Houston, Texas;* [3]*Picower Center for Learning and Memory and* [4]*Howard Hughes Medical Institute and Department of Brain and Cognitive Sciences, Massachusetts Institute of Technology, Cambridge, Massachusetts*

Submitted 1 June 2004; accepted in final form 27 August 2005

Jin, Dezhe Z., Valentin Dragoi, Mriganka Sur, and H. Sebastian Seung. Tilt aftereffect and adaptation-induced changes in orientation tuning in visual cortex. *J Neurophysiol* 94: 4038–4050, 2005. First published August 31, 2005; doi:10.1152/jn.00571.2004. The tilt aftereffect (TAE) is a visual illusion in which prolonged adaptation to an oriented stimulus causes shifts in subsequent perceived orientations. Historically, neural models of the TAE have explained it as the outcome of response suppression of neurons tuned to the adapting orientation. Recent physiological studies of neurons in primary visual cortex (V1) have confirmed that such response suppression exists. However, it was also found that the preferred orientations of neurons shift away from the adapting orientation. Here we show that adding this second factor to a population coding model of V1 improves the correspondence between neurophysiological data and TAE measurements. According to our model, the shifts in preferred orientation have the opposite effect as response suppression, reducing the magnitude of the TAE.

INTRODUCTION

The tilt aftereffect (TAE) is a striking visual illusion in which prolonged adaptation to an oriented visual stimulus causes subsequent stimuli to appear rotated away from the adapting orientation (Gibson and Radner 1937; He and MacLeod 2001; Magnussen and Johnsen 1986; Mitchell and Muir 1976). Explaining this and other aftereffects in terms of neural mechanisms has been an important outstanding problem. Historically, a popular explanation of the TAE has been a hypothesized relative suppression of neurons tuned to the adapting orientation (Clifford et al. 2000; Coltheart 1971; Sutherland 1961; Wainwright 1999). Recent physiological studies have confirmed that adaptation leads to suppression of neural responses near the adapting orientation. These experiments have also identified an additional effect of adaptation: the preferred orientations of neurons repulsively shift away from the adapting orientation (Dragoi et al. 2000, 2001). Here we construct a population coding model that includes both factors and show that the repulsive shifts of preferred orientations are important for quantitatively explaining the TAE. According to the model, the TAE is indeed caused by the relative suppression of neural responses. However, it is substantially weakened by the preferred orientation shifts. We suggest that the visual system uses the repulsive shifts of preferred orientations to reduce the perceptual error in orientation that could be induced by neural response suppression.

Quantitative measurements of the TAE are schematically summarized in the graph of Fig. 1*A*, which depicts the difference between the perceived and true orientation of a test stimulus as a function of the difference between the test and adapting orientations. According to this graph, the perceived orientation is similar to the true orientation, but rotated away from the adapting orientation by up to 4 deg (Clifford et al. 2000; Gibson and Radner 1937; Magnussen and Johnsen 1986; Mitchell and Muir 1976). That is, the adapting orientation "repels" the perceived orientation.

Neurons in the primary visual cortex (V1) respond selectively to the orientation of a stimulus (Hubel and Wiesel 1962). Orientation selectivity is generally characterized by a tuning curve depicting the firing rate of a neuron as a function of stimulus angle. Two major changes in tuning curves of VI neurons are observed after adaptation, particularly when the adapting orientation is close to a cell's preferred orientation (Dragoi et al. 2000) (Fig. 1*B*). First, the amplitude of the tuning curve on the flank near the adapting orientation depresses after adaptation; this is often accompanied by an increase in response amplitude on the opposite or far flank. Second, the location of the peak response, or preferred orientation of the cell, shifts away from the adapting orientation, so that the effect is "repulsive." The amount of the shift, which depends on the difference between the preferred and the adapting orientations, can be on the order of 10 deg (Dragoi et al. 2000) (Fig. 1*B*).

To show that the adaptation-induced changes of the tuning curves of V1 neurons are quantitatively consistent with the TAE, we mathematically analyze a population coding model. Similar to previous models (Clifford et al. 2000; Gilbert and Wiesel 1990; Pouget et al. 2000; Vogels 1990; Wainwright 1999), our model assumes that the population response profile of V1 neurons to a stimulus determines its perceived orientation. The analysis unveils a quantitative relationship between adaptation-induced changes of the perceived orientations and those of the tuning curves: The amplitude suppression of the tuning curves near the adapting orientation is positively correlated with the sum of the repulsive shifts of perceived orientations and the preferred orientations of neurons. We use this quantitative relationship to check the consistency between the psychophysical and physiological data. From the measured amount of the TAE and the shift of the preferred orientations, we predict the response suppression of the tuning curves near

Address for reprint requests and other correspondence: D. Jin, Department of Physics, The Pennsylvania State University, 104 Davey Lab, PMB #206, University Park, PA 16802 (E-mail: djin@phys.psu.edu).

The costs of publication of this article were defrayed in part by the payment of page charges. The article must therefore be hereby marked "*advertisement*" in accordance with 18 U.S.C. Section 1734 solely to indicate this fact.

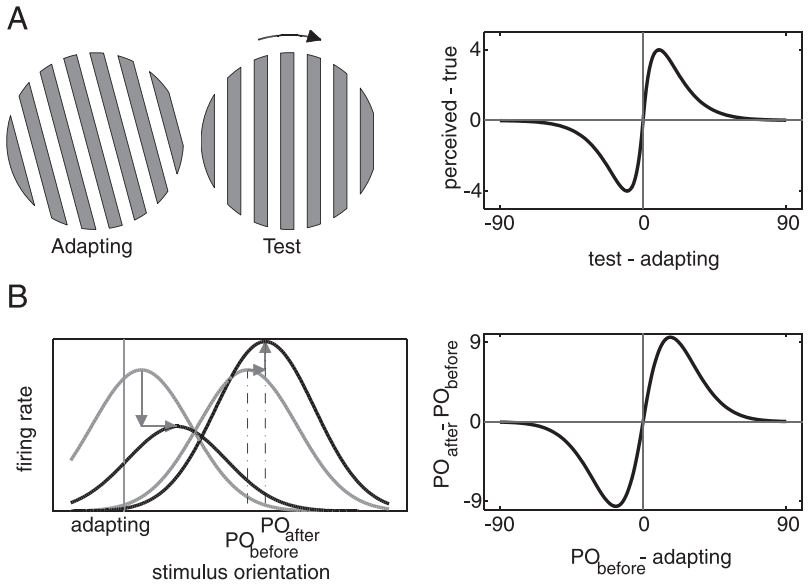

FIG. 1. Summary of psychophysical and physiological data related to the effects of orientation adaptation. *A*: prolonged adaptation to a tilted grating (*left*) causes the vertical grating (*right*) to appear rotated away from the orientation of the adaptor (Gibson and Radner 1937; He and MacLeod 2001; Magnussen and Johnsen 1986; Mitchell and Muir 1976). *Right*: curve schematically summarizes the difference between the true and adapting orientations. *B*: prolonged adaptation to a grating causes repulsive shifts of the preferred orientations of neurons in primary visual cortex (V1) (Dragoi et al. 2000). *Left*: tuning curves of 2 neurons. For each neuron, the gray curve represents the tuning curve of a neuron before adaptation. Black curve is the tuning curve after adaptation. Adapting orientation is represented by the gray vertical line. Preferred orientation shifts repulsively away from the adapting orientation (horizontal arrows). Amplitude of the tuning curve also changes. For the neuron with preferred orientation close to the adapting orientation, the amplitude diminishes (left vertical arrow). For the neuron with preferred orientation far from the adapting orientation, the amplitude may increase (right vertical arrow). *Right*: curve schematically summarizes the difference between the preferred orientation after adaptation and the preferred orientation before adaptation as a function of distance between the preferred and adapting orientations.

the adapting orientation. This prediction is then compared with the observed response suppression. The results confirm that the TAE is quantitatively consistent with the measured changes of tuning curves of V1 neurons under adaptation. The relationship further illustrates that, for a given response suppression, the repulsive shift of the preferred orientation reduces the amount of the TAE and thus the perception error.

The relationship between the changes of the orientation tuning curves and those of the orientation perceptions has been discussed *qualitatively* before (Clifford et al. 2000; Coltheart 1971; Gilbert and Wiesel 1990; Sutherland 1961; Teich and Qian 2003; Wainwright 1999; Yao and Dan 2001). However, such qualitative discussions cannot resolve the issue of the consistency between the adaptation-induced changes of the tuning curves and the TAE; a *quantitative analysis* is necessary. Our novel mathematical analysis enables the quantitative comparison between the physiological and psychophysical data.

METHODS

Experimental data

In this paper we use data from physiological and psychophysical experiments documented previously. Here we briefly describe these experiments. In the physiological experiments (Dragoi et al. 2000), the orientation tuning curves of neurons in V1 of anesthetized cats were measured by presenting high-contrast square-wave drifting gratings at 16 orientations (equally spaced at 22.5 deg), and recording the spike trains. The gratings had a spatial frequency of 0.5 cycle/deg, and temporal frequency of 1 Hz. Before adaptation, each orientation was presented for ten trials, with each trial lasting 2.5 s. Neuron spike rates were averaged over trials for each orientation. Adaptation was induced by presenting a drifting grating at the adapting orientation for 2 min. After adaptation, each of the 16 orientations was presented for 112 trials, with each trial lasting 2.5 s, preceded by a 5-s presentation of the adapting orientation to maintain the effects of adaptation.

In the psychophysical experiments that measured the TAE (Clifford et al. 2000, 2003) human subjects were presented with contrast reversing, stationary sinusoidal gratings with spatial frequency 1 cycle/deg and temporal frequency 1 Hz. The TAE was measured using adapting stimuli at six orientations of equal spacing of 15 deg. Each adapting stimulus was presented for 1 min. After adaptation, the perceived vertical orientation was measured using test stimuli with orientations progressively closer to the subjects' judgment of vertical orientation. Each testing stimulus lasted 400 ms followed by a 5-s presentation of the adapting stimulus to maintain the effects of adaptation. The test stimuli were presented for 60 trials. The difference between the true and perceived vertical orientation was the TAE.

The model

The central feature of our model is the *rate function,* which is a compact description of the tuning curves of the neuronal population. Our goal is to show how the activity of the neuron population, as defined by the rate function, changes as a result of the response suppression and orientation shift of tuning curves. We describe three different procedures for calculating, through the rate function, the relationship between the changes of the tuning curves and those of population responses, and illustrate our results in detail with one method, the winner-take-all method (see APPENDIX). We then show that the other two methods, the population vector method and the maximum-likelihood method, lead to similar results.

RESULTS

Orientation perception is commonly presumed to arise from the population responses of V1 neurons to oriented stimuli (Clifford et al. 2000; Gilbert and Wiesel 1990; Pouget et al. 2000; Vogels 1990; Wainwright 1999). From this perspective, it is straightforward to see how adaptation-induced changes in the tuning curves of V1 neurons lead to errors in orientation perception because such changes alter the population response profiles of V1 neurons. Thus, the neural basis of the TAE is simple to grasp qualitatively. However, it is not obvious that the specific changes of tuning curves observed in physiological experiments (Dragoi et al. 2000) are quantitatively compatible with the TAE. The experiments show that the preferred orientations of neurons shift away from the adapting orientation; moreover, maximum firing rates are reduced especially for neurons with preferred orientations near the adapting orientation. Do these changes lead to shifts of the perceived orientation away from the adapting orientation, as in the TAE? Moreover, are the amounts of change of tuning curves consistent with the magnitude of perception shifts in the TAE? We

address these questions by mathematically analyzing the relationship between the changes of tuning curves and those of orientation perception in a population coding model.

To do this, two issues about population coding models must be addressed. The first issue concerns the diversity of orientation tuning properties of V1 neurons. Tuning curves of V1 neurons, even for those with the same preferred orientations, may have quite different widths and maximum rates (Hubel and Wiesel 1962). Such diversity makes our mathematical analysis difficult. We overcome this difficulty by replacing all neurons of the same preferred orientation with a single "representative neuron." The tuning curve of this single neuron is the average of those of the neurons with the same preferred orientation. Thus, in our population coding model, there is one neuron for each preferred orientation. Before adaptation, the tuning curves of all neurons have the same Gaussian shape. Each neuron is labeled with its preferred orientation in the unadapted state. After adaptation, the tuning curves remain Gaussian; however, the preferred orientations may shift from the neuron labels. Moreover, the amplitudes and the widths of the tuning curves may change as well.

The second issue concerns how the rest of the brain "reads out" orientation from V1 neuron responses. This is not a settled matter in population coding models in general (Pouget et al. 2000). Among many possible proposals, three methods are commonly used in the literature: the winner-take-all, the population vector, and the maximum-likelihood methods. In the winner-take-all method, the perceived orientation is set to the label of the neuron that fires maximally to the stimulus. In the population vector method (Georgopoulos et al. 1982; Gilbert and Wiesel 1990; Vogels 1990), each neuron contributes a two-dimensional vector with orientation equal to twice its label and length equal to its firing rate; summation of these vectors results in a population vector, whose orientation is taken as twice the perceived orientation. In the maximum-likelihood method (Paradiso 1988; Pouget et al. 2000), each perceived orientation is associated with a predetermined template of population responses. These templates are compared to the population response to a stimulus and the one that best matches determines the perceived orientation. In our analysis of the neural basis of the TAE, we use all three methods and show that they lead to similar results. The winner-take-all method is the simplest and is amenable to mathematical analysis; we therefore explain our results mostly in terms of this readout method. The results from the other two methods are presented later and compared.

Before presenting the detailed quantitative analysis, we explain qualitatively how adaptation-induced changes of tuning curves are related to the TAE. We first examine the two types of changes—response suppression and orientation shift—separately, and then combine them. Without loss of generality, we assume that the adapting orientation is at $\theta_1 = 0$.

Figure 2*A* shows that the suppression of tuning-curve amplitudes near the adapting orientation causes repulsive shifts of the perceived orientations, which is the essence of the fatigue model of TAE (Clifford et al. 2000; Coltheart 1971; Sutherland 1961; Wainwright 1999). Consider the population response to

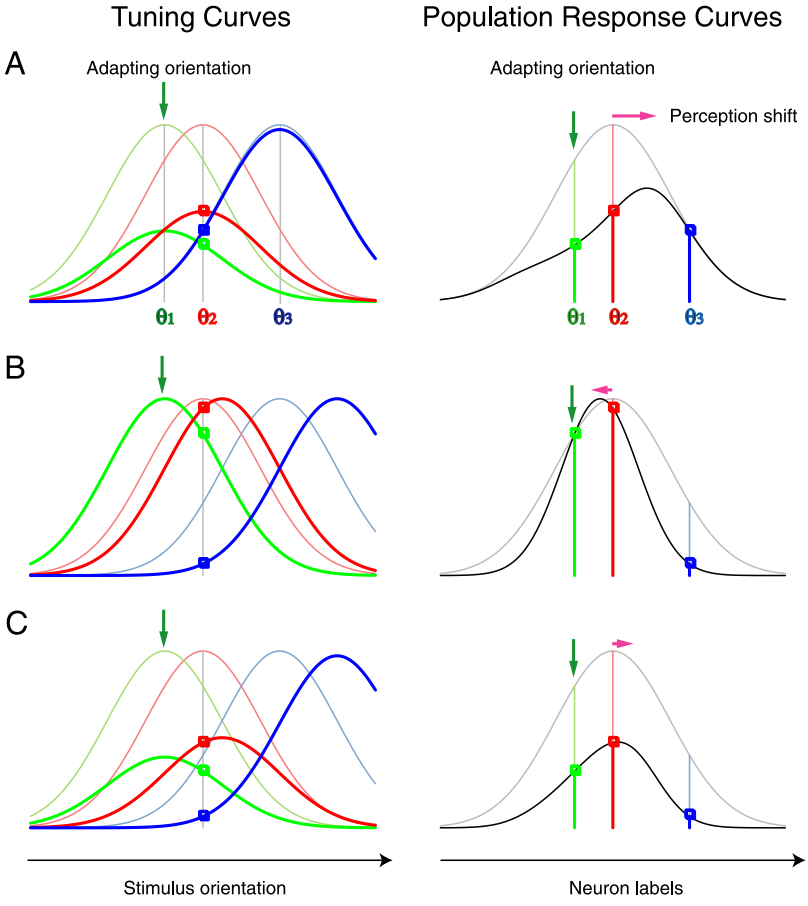

FIG. 2. Relationship between changes of tuning curves and shifts of perception. *Left*: tuning curves of 3 neurons with preferred orientations at $\theta_1 = 0 < \theta_2 < \theta_3 < 90$ (indicated in green, red, and blue, respectively) before adaptation. Thin lines are tuning curves before adaptation, whereas thick lines are those after adaptation. Green arrows indicate the adapting orientation θ_1. Colored dots indicate the firing rates of each neuron to a test stimulus at θ_2 after adaptation. *Right column*: population response curves to the test stimulus. Population curves before and after the adaptation are indicated with thin gray and thick black lines, respectively. Green arrows indicate the adapting orientation. Colored vertical lines indicate the firing rates of the green, red, and blue neurons, respectively, and the colored dots indicate the firing rates of the neurons after adaptation. Perceived orientations are given by the maxima of the population response curves. Pink arrows indicate the directions and magnitudes of shifts of the perceived orientations after adaptation. *A*: adaptation induces only amplitude suppression of the tuning curves. Amplitude suppression is progressively smaller because the preferred orientation of the neuron is further away from the adapting orientation. Consequently, the population response curve shifts away from the adapting orientation, resulting in a repulsive shift of the perceived orientation, as in the tilt aftereffect (TAE). *B*: adaptation induces only repulsive shifts of preferred orientations of neurons, which makes the peak of the population response curve shift toward the adapting orientation, leading to an attractive shift of the perceived orientation, contrary to the TAE. *C*: adaptation induces both amplitude suppression and repulsive shifts of preferred orientations. Opposing effects of these 2 changes on the perceived orientation leads to a smaller total shift of the perceived orientation than that with suppression alone.

a test stimulus at $\theta_2 > \theta_1 = 0$. Before adaptation, the neuron with label θ_2 responds maximally to the stimulus because its preferred orientation matches the stimulus orientation; and neurons with labels equidistant to θ_2 have the same firing rates because their tuning curves are identical in shape and symmetric around the neuron label. Thus the population response curve, which describes the firing rates of neurons to the stimulus θ_2 as a function of their labels, is symmetric around θ_2; and the perceived orientation of the stimulus is θ_2. After adaptation, the firing rates of neurons with labels in between the adapting and the test orientations are suppressed more than those with labels larger than the test orientation. This asymmetric suppression leads to a skewed population response profile with the peak position larger than θ_2, which causes a repulsive shift of the perceived orientation.

Figure 2*B* shows that the repulsive shift of preferred orientation leads to attractive shift of the perceived orientation, as has been discussed in previous qualitative studies (Gilbert and Wiesel 1990; Teich and Qian 2003; Yao and Dan 2001). Consider the firing rate of neuron θ_2 to the test stimulus at θ_2. Before adaptation, this neuron has the maximum firing rate compared to that of other neurons. After adaptation, its preferred orientation shifts to an orientation larger than θ_2. The test stimulus is no longer at the preferred orientation and the neuron's firing rate drops. The firing rates of all neurons with labels $>\theta_2$ also drop because the repulsive shifts make the test orientation farther away from the new preferred orientations. The situation is different for the neurons with labels between 0 and θ_2; the firing rates of some of them actually go up because the test orientation is now closer to the new preferred orientations. These asymmetric changes of firing rates lead to a skewed population response profile with peak position $<\theta_2$, which causes an attractive shift of the perceived orientation, opposite to the TAE.

The above discussion demonstrates that the amplitude suppression and repulsive shift of preferred orientations have opposite effects on how the population response and thus the perceived orientation shifts. When both types of change coexist, the direction of the perception shift depends on which type predominates. Figure 2*C* shows that, if the amplitude suppression predominates, the perceived orientation shifts repulsively as in the TAE, but the magnitude of the shift is smaller than that with the amplitude suppression alone. On the other hand, if the repulsive shift dominates, the perceived orientation shifts attractively, opposite to the TAE. Which directions of perception changes are predicted by the physiological data, and whether the data are consistent with the TAE, can be addressed only through quantitative analysis of the relative contributions of the two types of change.

A straightforward way of accessing the consistency between the physiological data and the TAE is as follows: Construct tuning curves of the V1 neurons after adaptation using the measured amplitude suppressions and preferred orientation shifts, obtain the population response profiles to all stimulus orientations, and calculate the resulting shifts of the perceived orientations, as shown in Fig. 2*C* for one stimulus. This approach, although intuitive and simple however, is not the best way of quantitatively checking the consistency because the two types of change lead to opposite effects on the perceived orientation. This situation is analogous to experimentally checking whether the relationship $A = B - C$ holds for three positive variables *A, B, C,* with *A* much smaller than *B* and *C*. Data on these quantities are inevitably noisy. In general, the variance of data is positively correlated to the mean, unless the measurements are controlled to high precision; thus, it is reasonable to assume that var (*B*) and var (*C*) are much larger than var (*A*). Note that var $(B - C)$ = var (*B*) + var (*C*) and is much larger than var (*A*). Thus, the mean of $B - C$ can be buried by the variance and is not easily compared to data on *A*. A better way is to check the equivalent relationship $B = A + C$. Here, var $(A + C)$ = var (*A*) + var (*C*). However, because var (*A*) is much smaller than var (*C*), the variance of the sum is not too much larger than var (*C*) and is comparable to var (*B*). Thus, the mean of $A + C$ is not buried by the variance, which makes checking the relationship $B = A + C$ far more reliable.

A way of checking the consistency between the physiological data and the TAE, which is analogous to checking the relationship $B = A + C$ discussed above, is as follows: Use the measured repulsive shifts of the preferred orientations and the measured TAE to predict the required amount of amplitude suppressions of the tuning curves and compare the prediction to the data. This approach takes advantage of the small variance of the TAE measurement (Clifford et al. 2000). In the following, we derive a mathematical relationship that relates the shifts of the preferred orientations and the TAE to the amplitude suppressions. This relationship is then used to verify the consistency between the physiological data and the TAE.

We first define symbols and functions that are useful for our analysis. As stated previously, each neuron in the population has a label, which is its preferred orientation ψ in the unadapted state. It should be emphasized that ψ is an invariant label. After adaptation, the label of each neuron remains the same as before adaptation, even though its preferred orientation may change substantially. The *rate function* $F(\psi, \phi)$ is defined as the firing rate of neuron ψ to a stimulus with orientation ϕ. Note that the two Greek letters are mnemonic. Because the orientation of the stimulus is a "physical" quantity, it is denoted by the letter ϕ ("phi"). The label of a neuron is a "psychic" quantity, so it is denoted by the letter ψ ("psi"). When considered as a function of the stimulus orientation ϕ only, *F* is the tuning curve of the neuron with label ψ. When considered as a function of the neuron label ψ only, *F* is the population response to a stimulus with orientation ϕ. Therefore the rate function *F* is a complete description of both population responses and tuning curves. The rate function can be visualized with a three-dimensional graph of firing rate versus neuron label and stimulus orientation (Fig. 3). Two curves on the surface of the rate function are convenient to define. The first is the *perception line* $\psi_p(\phi)$, which marks the perceived orientation of stimulus ϕ. In the winner-take-all method, $\psi_p(\phi)$ is computed by maximizing the rate function $F(\psi, \phi)$ with respect to the neuron label ψ for fixed stimulus orientation ϕ. The second is the *neuron line* $\phi_n(\psi)$, which marks the preferred orientation of neuron ψ, and is the maximum of the rate function $F(\psi, \phi)$ with respect to the stimulus orientation ϕ for fixed neuron label ψ. Before adaptation, $\phi_n(\psi)$ is equal to ψ, although it may shift after adaptation.

Figure 3 illustrates the relationship between the rate function (*left*) and the neuron and perception lines (*right*) in various situations. Both the population responses (blue) and tuning curves (red) are shown in the left graphs. The maxima of the

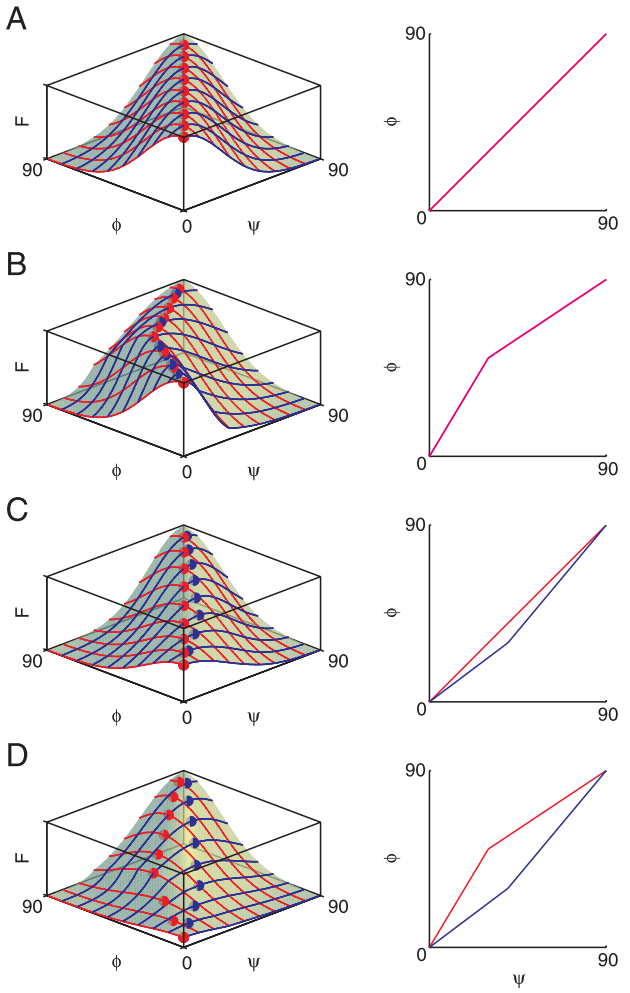

FIG. 3. Relationship between changes of tuning curves and shifts of perception explained with the rate function. *Left*: plots of the rate functions. Each point on the surface of a rate function represents the firing rate of a neuron at one stimulus orientation. Here ψ is the neuron label and ϕ is the stimulus orientation. Only the part of the rate functions for $0 < \psi < 90$ and $0 < \phi < 90$ is shown. Adapting orientation is at 0. Red lines are tuning curves and blue lines are the population response curves. Red and blue dots indicate maxima of the tuning and population response curves, respectively. *Right column*: plots of the lines of the perceived orientations (blue) and the preferred orientations (red). Lines correspond to the rate function on the *left* in the following way: the red line represents the locations of the peaks of the tuning curves and the blue line represents the locations of the peaks of the population response curves. Magenta lines indicate that the red and blue lines coincide. Only the parts for $0 < \psi < 90$ are shown. *A*: before adaptation. Tuning curves all have the same Gaussian shape, and the preferred orientations are the same as the neuron labels. Peaks of tuning curves and population curves coincide. There is no shift of perception. *B*: preferred orientations shift repulsively (i.e., they are further away from the adapting orientation compared to their values in the unadapted state), whereas the amplitudes remain uniform. Peaks of tuning curves and population curves still coincide. Perceived orientations shift attractively, contrary to the TAE. *C*: preferred orientations do not shift, but the amplitudes suppress near the adapting orientation. Peaks of tuning curves and population curves no longer coincide. Perceived orientations shift repulsively, as in the TAE. *D*: preferred orientations shift repulsively and the amplitudes suppress near the adapting orientation. Suppression is much stronger than in *C*. This is needed to produce the same amount of repulsive shift of the perceived orientations as in *C*.

blue curves in the left graph define the perception line, which is plotted on the *right* in blue as a graph of $\psi_p(\phi)$ versus ϕ. The maxima of the red curves in the left graph define the neuron line, which is plotted on the *right* as a graph of $\phi_n(\psi)$ versus ψ.

The results of Fig. 3 are the same as those of Fig. 2, but explained differently through the rate function. This approach further leads to a quantitative understanding of the effects of the tuning curve changes on orientation perception.

Figure 3*A* shows the rate function before adaptation, which looks like a ridge that is diagonally oriented in the ψ–ϕ plane (Fig. 3*A*, *left*). The perception and neuron lines coincide exactly at the top of the ridge, which means that perceived orientations are the same as true orientations. When the lines are plotted in two dimensions, they both lie along the diagonal (Fig. 3*A*, *right*).

The rest of Fig. 3 illustrates the rate function after adaptation. As in Fig. 2, it is helpful to first examine the cases of each change happening in isolation (Fig. 3, *B* and *C*), then proceed to the case of both changes happening simultaneously (Fig. 3*D*). As before, we assume that the adapting stimulus is oriented at 0 deg.

In Fig. 3*B*, the preferred orientations shift after adaptation, with no change in tuning-curve amplitudes. In the rate function on the *left,* the preferred orientations are the maxima of the red curves. The neuron line [preferred orientation $\phi_n(\psi)$ vs. neuron label ψ] is plotted on the *right* (red). It is shifted away from the diagonal. The shift vanishes at 0 and 90 deg and is maximal at an intermediate orientation. Similar shifts are observed experimentally in V1 neurons after adaptation (Dragoi et al. 2000). Because the height of the ridge is constant, the maxima of the blue curves lie along the same line as the maxima of the red curves. Consequently the perception line (blue) coincides with the neuron line; both are identically shifted away from the diagonal. The shift in the neuron line is repulsive [$\phi_n(\psi) > \psi$], whereas the shift in the perception line is attractive [$\psi_p(\phi) < \phi$].

In Fig. 3*C*, the tuning-curve amplitudes are suppressed for neurons tuned near the adapting orientation, causing the ridge of the rate function to be depressed near the origin. There is no shift in preferred orientations, however, so the neuron line lies along the diagonal, as in the unadapted state of Fig. 3*A*. Because of the lowered ridge height, the maxima of the blue curves shift away from the diagonal. As shown on the *right,* the perception line shifts repulsively [$\psi_p(\phi) > \phi$]. In other words, suppression alone can induce repulsive shifts of perception.

Figure 3*D* illustrates the effect of combining both suppression and shift, which corresponds to what is observed experimentally in V1. The neuron and perception lines both shift repulsively. To produce the same perceptual shift as in Fig. 3*C*, a stronger suppression of the ridge near the origin is necessary to produce the repulsive shift of the preferred orientation (compare to the rate function of Fig. 3*C*). The stronger amplitude suppression counteracts the weakening effect of the repulsive shift of the preferred orientation on the TAE.

In Fig. 3*B*, the neuron and perception lines coincided exactly, and there was no change in the tuning-curve amplitudes. In Fig. 3, *C* and *D*, there was a separation between the neuron and perception lines, and the tuning-curve amplitudes were suppressed near the origin. Figure 4 presents a graphical "proof" that separation between the neuron and perception lines is necessarily accompanied by suppression of tuning-curve amplitudes. Consider a path that travels from the red neuron line (point 1) to the blue perception line (point 2) back to the red neuron line (point 3). We will prove that the rate function is larger at point 1 than at point 3. The vertical path

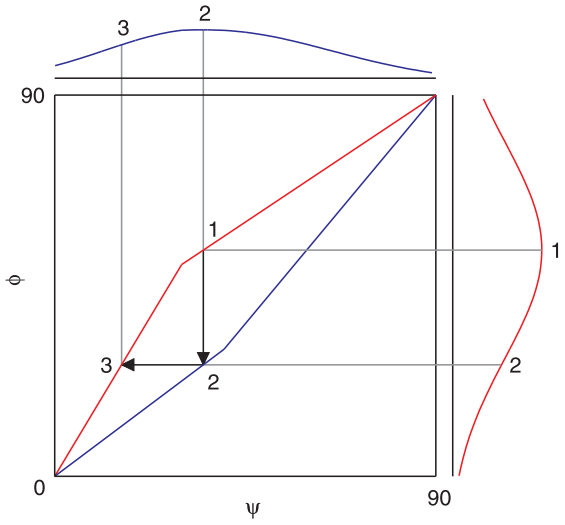

FIG. 4. Graphic "proof" that repulsive shift of preferred and perceived orientations is necessarily accompanied by suppression of tuning-curve amplitudes. In the box, the red line indicates the preferred orientation for the neuron with label ψ and is termed *the neuron line;* the blue line indicates the perceived orientation for the stimulus at orientation ϕ and is termed *the perception line.* Consider a path that travels from the red neuron line (point 1) to the blue perception line (point 2) back to the red neuron line (point 3). We show that firing rate is larger at point 1 than that at point 3. Vertical path from 1 to 2 travels along the ϕ direction and therefore traces out the tuning curve of some neuron, which is graphed to the *right* of the box. Because 1 is on the neuron line, it corresponds to the maximum of the tuning curve; therefore the firing rate at 1 is larger than that at 2. Horizontal path from 2 to 3 travels along the ψ direction and therefore traces out the population response for some orientation, which is graphed above the box. Because 2 is on the perception line, it corresponds to the maximum of the population response; therefore the firing rate is larger at 2 than that at 3. It follows that the firing rate at 1 is larger than that at 3. This downhill path can be continued, alternating between the neuron and perception lines, proving that tuning-curve amplitudes are suppressed near the origin. This suppression is large if the distance of the path is long or, equivalently, the repulsive shifts of the preferred orientations and the perceived orientations are large. Narrow tuning curves or population response curves have a similar effect.

from 1 to 2 travels along the ϕ direction and therefore traces out the tuning curve of some neuron, which is graphed to the *right* of the box. Because 1 is on the neuron line, it corresponds to the maximum of the tuning curve, and thus the rate function at 1 is larger than that at 2. The horizontal path from 2 to 3 travels along the ψ direction, and therefore traces out the population response for some orientation, which is graphed above the box. Because 2 is on the perception line, it corresponds to the maximum of the population response. Therefore the rate function is larger at 2 than at 3. It follows that the rate function at 1 is larger than that at 3. This downhill path can be continued, alternating between the neuron and perception lines, proving that tuning-curve amplitudes are suppressed near the origin.

The arguments of Fig. 4 can be made quantitative. The general idea is to specify the neuron and perception lines and then derive the amount of amplitude suppression that is required. This calculation can be done by modeling the rate function as

$$F(\psi, \phi) = A(\psi) \exp\left\{ -\frac{[\phi - \phi_n(\psi)]^2}{2\sigma(\psi)^2} \right\} \quad (1)$$

Here the tuning curve of neuron ψ is Gaussian with amplitude $A(\psi)$, width $\sigma(\psi)$, and preferred orientation $\phi_n(\psi)$. The functions $\phi_n(\psi)$ and $\sigma(\psi)$ are determined by neural data, whereas the perception line $\psi_p(\phi)$ is determined by TAE data. From *Eq. 1* it follows that (see APPENDIX for derivation)

$$A(\psi) = \exp\left\langle \int_0^{\psi} d\psi' \frac{[\phi_n(\psi') - \psi_p^{-1}(\psi')]}{\sigma(\psi')^2} \left\{ \frac{d\phi_n(\psi')}{d\psi'} - \frac{[\phi_n(\psi') - \psi_p^{-1}(\psi')]}{\sigma(\psi')} \frac{d\sigma(\psi')}{d\psi'} \right\} \right\rangle \quad (2)$$

Here $\psi_p^{-1}(\psi')$ is the inverse function of the perception line. The formula allows the possibility that the widths of tuning curves vary for different neurons. The adapting orientation is at 0. This formula was used to construct Fig. 3. It will also be used in the remainder of this paper, which will quantitatively compare this predicted amplitude from the model with the tuning-curve amplitudes measured experimentally in V1 neurons.

To illustrate *Eq. 2* in simple terms, we further simplify it with two approximations. First, the tuning curves of different neurons are assumed to have the same width, although this width may change after adaptation. Second, the neuron and perception lines are approximated as piecewise linear. The approximate lines coincide with the original neuron and perception lines at the origin or 0 deg (the adapting orientation), at 90 deg (orthogonal to the adapting orientation), and at locations of maximal shifts, respectively. These approximations allow us to explicitly express the amplitude of the tuning curves as a function of five parameters: the width parameter σ of the tuning curves; the location Φ and magnitude δ of the maximum repulsive shift of the perceived orientations; and the location ψ and magnitude Δ of the maximum repulsive shift of the preferred orientations (see APPENDIX for details). The amplitude $A(\psi)$ of the tuning curve for neuron ψnear the adapting orientation at 0 is approximately given by the following expression

$$A(\psi) \approx \exp\left[\left(\frac{\Delta}{\Psi} + \frac{\delta}{\Phi} \right) \frac{\psi^2}{2\sigma^2} \right] \quad (3)$$

This formula succinctly summarizes how the amplitude of the tuning curves depends on the shifts of the perception and the preferred orientation. As the neuron label ψ goes further away from the adapting orientation at 0, the amplitude grows exponentially; the rate of the growth is proportional to the sum of the repulsive shifts of the perceived and the preferred orientations and is inversely proportional to the width of the tuning curves. The rise of the amplitude is more pronounced for large Δ compared to the case of $\Delta = 0$ (i.e., no shift of preferred orientation), as illustrated in Fig. 3, *D* and *C*.

The analytical result of *Eq. 3* was derived from *Eq. 2* using piecewise-linear approximations for the perception and neuron lines. We can also do the same calculation numerically, using the perception line and neuron line determined by the data. Fitting with fourth-order polynomials, we determine the perception line $\psi_p(\phi)$ from the psychophysical data on the TAE (Clifford et al. 2000) (Fig. 5*A*); fitting with a straight line, we determine the neuron line $\phi_n(\psi)$ from the physiological data (Dragoi et al. 2000) (Fig. 5*B*). In the physiological experiments, adaptation also changes the width of the tuning curves, as evident from the changes of the orientation selectivity indices (OSIs) (Dragoi et al. 2000). We convert the data on the

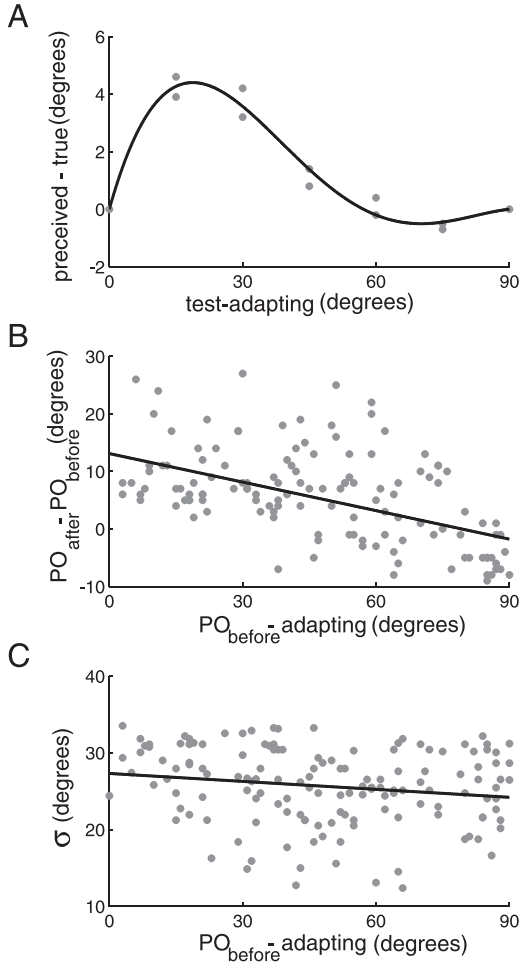

FIG. 5. Least-squares fits of experimental psychophysical and physiological data. *A*: amount of repulsive shift of the perceived orientation is plotted against the difference between the testing orientation and the adapting orientation. Gray dots are the psychophysical experimental data taken from Clifford et al. (2000). Black curve is the least-square fit of the data to a polynomial of the form $\phi(90 - \phi)a(1 + b\phi)(1 + c\phi)$. Fitting parameters are $a = 0.0061$, $b = -0.011$, $c = -0.017$. *B*: amount of repulsive shift of the preferred orientation is plotted against the difference between the neuron label and the adapting orientation. Gray dots are taken from the physiological experimental data of Dragoi et al. (2000). Black curve is the least-square fit of the data to a line of the form $a + b\psi$, with parameters $a = 13$, $b = -0.17$. *C*: tuning width parameter is plotted against the difference between the neuron label and the adapting orientation. Gray dots are adapted from the orientation tuning index data of Dragoi et al. (2000). Black line is a least-squares fit of the data to a line of the form $a + b\psi$, with the parameters $a = 27$, $b = -0.34$.

OSIs to that on the width parameters assuming a linear relationship between the OSIs and the width parameter (Swindale 1998). The relationship is determined by two points: the width parameter is zero when OSI is 1 and the averaged half-width of tuning curves before adaptation is 30 deg (Watkins and Berkley 1974). We fit the converted data on the width parameters with a straight line (Fig. 5*C*).

Using the experimentally determined perception and neuron lines and tuning width parameters, we calculate the amplitude of the tuning curves using *Eq. 2*. The calculated amplitude curve is plotted in Fig. 6, *left* (red curve). We compare this curve with physiological data on the amplitude changes of the tuning curves, which are calculated by taking the ratios of the observed maximum firing rates of neurons after and before adaptation (the green circles with error bars in Fig. 6). [These data are derived from neurons studied by Dragoi et al. (2000), but are presented in this form for the first time. The spontaneous firing rates are subtracted before calculating the ratios.] The overall scaling of the amplitude curve is not determined in the theory; we therefore scaled the curve to best match the experimental data. The comparison is in rough quantitative agreement (sum of square difference to the data points divided by variance, or chi-square $\chi^2 = 0.27$; χ^2 test of the hypothesis that there is no difference between the data and the prediction $p = 1 - 0.002$; degree of freedom for χ^2 test is 5).

To see whether the observed changes of the tuning curves, in particular whether the shifts in preferred orientation, are essential for agreement between the theory and the data, we calculated the amplitude curve using the perception line from the psychophysical data but assuming no shifts of the preferred orientations. The results are plotted in Fig. 6, *right* (dotted red line). The comparison is clearly not as good as that with the preferred orientation shifts ($\chi^2 = 0.83$, $p = 1 - 0.02$).

To summarize, we have compared two models, one that includes the repulsive shifts of preferred orientation and one that does not. Figure 6 shows that the model with preferred orientation shifts explains the data better. This is not the result of fitting extra parameters to produce better agreement in Fig. 6 because the preferred orientation shifts are determined by an

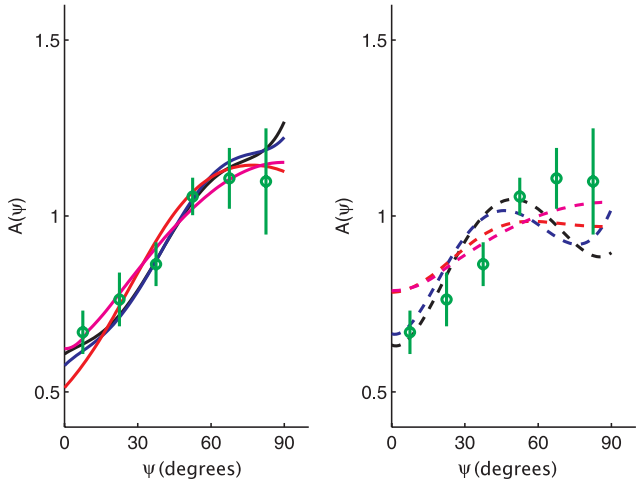

FIG. 6. Consistency of model results with physiological and psychophysical data on adaptation. From the physiological data, we calculate the ratio of the amplitudes of the tuning curves after and before adaptation, after subtraction of the spontaneous firing rates (adapted from Dragoi et al. 2000). Green circles are obtained by averaging these ratios within 15-deg bins, and the error bars represent SE. Curves are the theoretical calculations of the ratio as a function of the difference between the neuron label (i.e., preferred orientation before adaptation) and the adaptation orientation. Theoretical curves are scaled to minimize the square error relative to the data. Curves are color-coded to indicate the population coding methods used: winner-take-all (red and magenta), population vector (black), and maximum-likelihood (blue). *Left*: solid curves on the *left* are calculated with repulsive shifts of *both perceived and preferred orientations,* as in Fig. 4*D*. Except the magenta curve, all curves are calculated using the results shown herein for shifts of the perceived and preferred orientations, as well as the changes of the tuning width. Magenta curve is calculated using the piecewise linear approximations to the shifts, and a constant tuning width. *Right*: dotted curves on the *right* are calculated with the shifts of the perceived orientations, *but without the repulsive shifts of the preferred orientations,* as in the model of Fig. 4*C*. Curves on the *left* are more consistent with the physiological data than those on the *right.* For the amount of the TAE measured in psychophysical experiments, the repulsive shifts of preferred orientations are necessary for better explaining the observed amount of relative suppression of the tuning curves.

independent fit to data in Fig. 5*B*. In both the *left* and *right panels* of Fig. 6, there is only a single free parameter, an overall scale factor.

These results do not depend on either the exact shapes of the perception and the neuron lines or the variations of the tuning width. This is evident from the results that use the formula assuming piecewise-linear approximations of the perception and neuron lines and a constant width for the tuning curves (the formula is given in *Eqs. A7* and *A8* in the APPENDIX). The case with the repulsive shifts is plotted in Fig. 6, *left* (magenta curve, $\chi^2 = 0.057$, $p = 1 - 0.00004$) and that without is plotted in Fig. 6, *right* (dotted magenta line, $\chi^2 = 0.65$, $p = 1 - 0.01$). The results with the approximations closely resemble those without. Parameters for the piecewise-linear approximations are as follows: the maximum perceived orientation shift is 4 deg when the testing and adapting angles are 15 deg apart (Clifford et al. 2000); the maximum preferred orientation shift is 10 deg when the neuron label and the adapting angle are 5 deg apart; and the half-width of the tuning curves is 30 deg (Watkins and Berkley 1974).

We conclude from these comparisons that the observed changes of the neuron tuning curves after adaptation are quantitatively consistent with the TAE measured psychophysically. Moreover, the repulsive shifts of the preferred orientations are especially important for a better quantitative explanation of the TAE.

So far we have presented results using the winner-take-all method for reading out perceived orientations from the population responses. Similar results are obtained using two other readout methods: the population vector and the maximum likelihood.

In the population vector method, the perceived orientation of a stimulus is constructed from the responses of all neurons. Each neuron is assigned a vector, with the length proportional to the neuron's firing rate, and the angle with the horizontal axis equal to twice that of the neuron label (the preferred orientation before adaptation). Summation of the vectors gives a population vector, whose angle is assigned as twice that of the perceived orientation. Mathematically, the perceived orientation of stimulus ϕ is expressed according to the following formula

$$\psi_p(\phi) = \frac{1}{2}\arctan\left[\frac{\int_{\phi-90}^{\phi+90} d\psi \sin(2\psi)F(\psi, \phi)}{\int_{\phi-90}^{\phi+90} d\psi \cos(2\psi)F(\psi, \phi)}\right] \quad (4)$$

This readout method is more complicated than the winner-take-all method, and it is not straightforward to describe closed-form mathematical expressions for the amplitude function $A(\psi)$. Nevertheless, we can approximately compute this function by following an optimization procedure.

This is done by parameterization of the amplitude function. For each parameter set, a unique amplitude function is determined. Using the amplitude function, the rate function is constructed from the tuning curves and is used to calculate the perceived orientations of all stimuli. The shifts of the perceived orientations relative to the true stimulus orientations are then compared with the psychophysical data. We search the parameter space until the best comparison is reached. Some parameters can lead to multipeaked population profiles for some stimuli, for which the population vector method breaks down (Pouget et al. 2000); we therefore exclude such parameters in the search.

Mathematically, the above procedure can be expressed as follows. We parameterize $A(\psi)$ with Chebyshev polynomials (Press et al. 1988) up to the fifth order, as below

$$A(\psi) = 1 + \sum_{k=1}^{5} a_k\left\{\cos\left[k \arccos\left(\frac{\psi - 45}{45}\right)\right] - \cos(180k)\right\} \quad (5)$$

Here a_k, $k = 1,\ldots,5$ are the parameters. For each set of parameters, the perception line $\psi_p(\phi, \{a_k\})$ is calculated through *Eqs. 5, 1,* and *4*. We search the parameter space to minimize the following error function

$$E(\{a_k\}) = \int_0^{90} d\phi[\psi_p(\phi, \{a_k\}) - \psi_{p,\,\mathrm{OBSERVED}}(\phi)]^2 + R(\{a_k\}) \quad (6)$$

Here $R(\{a_k\})$ is the regularization factor. This factor is introduced to restrict the solution in parameter space so that no multiple peaks are allowed in the population profiles for any stimulus orientation because the population vector method breaks down for multipeaked population profiles. The factor R is 0 if the population profiles for all stimuli are one-peaked; otherwise, R is assigned a large number so that the error is large. The exact value of this large number does not affect the results (in our calculations, the value of the number is 15). Minimization of the error function leads to an amplitude function that produces a perception line as close as possible to the one determined by the psychophysical experiments, with the constraints that the population activity profiles for all stimuli are one-peaked. We use Powell's method (Press et al. 1988) for minimizing the error function.

In Fig. 6, *left,* we show the result (black curve) obtained using the experimentally determined curves for the shifts of the preferred and perceived orientations as well as the width parameters (Fig. 5). The result is quite similar to that of the winner-take-all method (red curve in Fig. 6), and again compares well with the experimental data ($\chi^2 = 0.089$, $p = 1 - 0.0001$). We also calculated the amplitude function without repulsive shifts of the preferred orientations and changes of the tuning width, which is shown in Fig. 6, *right* (dotted black curve). The comparison with the data is less compelling than that with the preferred orientation shifts ($\chi^2 = 0.61$, $p = 1 - 0.01$).

The results using the maximum-likelihood method (the blue curve in Fig. 6, *left,* with repulsive shifts of the preferred orientations, $\chi^2 = 0.14$, $p = 1 - 0.0004$; and the dotted blue curve in Fig. 6, *right,* without, $\chi^2 = 0.70$, $p = 1 - 0.02$) are also quite similar to those of the winner-take-all method. In the maximum-likelihood method, the perceived orientation of a stimulus ϕ is determined by fitting the population profile with preset templates, which are the population profiles before adaptation. Each perceived orientation has a corresponding template. The template corresponding to a perceived orientation ϕ is a Gaussian function centered at ϕ with the width parameter σ. The fitting procedure minimizes the integral of the square error between the template and the population profile through scaling the maximum of a template. The label of the best-matched template is assigned as the perceived

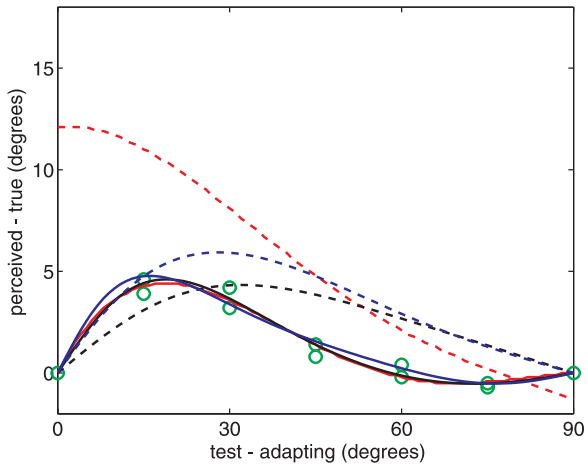

FIG. 7. Impact of repulsive shifts of the preferred orientations on accuracy of predicting TAE. Perceived orientation of a stimulus is calculated by obtaining population response profile from the rate function constructed using the adaptation-induced changes of tuning curves. Difference between the perceived and true orientations is the TAE. We use the amplitudes of the tuning curves as given in the *left graph* (the red, black, or blue curves for winner-take-all, population vector, or maximum-likelihood coding methods, respectively). Width parameters are given in the curve of Fig. 6*C*. Results with the repulsive shifts of the preferred orientations, as given in the curve of Fig. 6*B*, are plotted as the solid curves. Results with no shifts of the preferred orientations are plotted as the dotted curves. Red, black, or blue indicates that the population coding method use is winner-take-all, population vector, or maximum likelihood, respectively. Green circles are the psychophysical data (same as in Fig. 6*A*). Although the solid lines agree well with the data, the dotted lines do not. Including the repulsive shifts of preferred orientations is important for achieving accurate predictions of TAE with the given amplitude functions.

orientation. To calculate the amplitude function $A(\psi)$, we follow a numerical optimization procedure similar to that for the population vector-average method. A regularization factor is also similarly introduced because the maximum likelihood method is valid only for one-peaked population profiles just like the vector-average model.

The above results demonstrate that the TAE is consistent with adaptation-induced changes of the tuning curves of V1 neurons. The observed repulsive shifts of the preferred orientations after adaptation significantly contribute to such consistency. We can show this in another way: from the amplitude functions shown in the left graph of Fig. 6 (solid red curve for winner-take-all, solid black curve for population vector, or solid blue curve for maximum likelihood), we predict the TAE and compare to the psychophysical data. Specifically, we construct the rate function through *Eq. 1* with the amplitude function $A(\psi)$, the preferred orientations $\phi_n(\psi)$, and the width parameters $\sigma(\psi)$. From the rate function we obtain the population response profile for a given stimulus orientation and determine the perceived orientation using a population coding method (winner-take-all, population vector, or maximum likelihood). The difference between the perceived and true orientations of the stimulus is the predicted TAE. The width parameters are given in the curve plotted in Fig. 5*C*. We first calculate the TAE with the repulsive shifts of the preferred orientations, given in the curve of Fig. 5*B*. The results are plotted in Fig. 7, where the solid red, black, and blue curves are from winner-take-all, population vector, and maximum-likelihood coding methods, respectively. The calculated TAE agrees with the data (green circles, same as in Fig. 5*A*) quite well (the mean square root differences between the data and predictions are 0.36, 0.35, and 0.44, respectively). We then predict the TAE *with no shifts of the preferred orientations.* The results are plotted in Fig. 7, where the dotted red, black, and blue lines are from winner-take-all, population vector, and maximum likelihood, respectively. The calculated TAE does not agree with the data as well (the mean square root differences are 5.1, 1.8, and 2.3, respectively). Without the repulsive shifts of the preferred orientations, the predicted TAE is much larger than observed. The repulsive shifts of the preferred orientations thus contribute significantly to the consistency between adaptation-induced changes of orientation tuning and the TAE.

The amplitude $A(\psi)$ that predicts a TAE closest to the observed data is not a linear function, as shown in Fig. 6. However, given relatively large scatter of the physiological data on the amplitude suppression of tuning curves, shown in Fig. 6 as binned average and in Fig. 8*A* as scatter, such deviations from linearity might be hard to distinguish statistically. Thus, it is instructive to calculate the predicted TAE with the amplitude function obtained by fitting straight lines to the suppression data, as shown in Fig. 8*A*, and compare to data the predicted TAE with and without repulsive shifts of preferred orientations. Lines with slopes within a range all fit well with the amplitude data, as shown in Fig. 8*A*, where we shown three fitted lines. The red line is the result of least-square fit to the data and the black and blue lines are with the slope increased or decreased by 1 SE of the slope estimated in the least-square fit, respectively. The lines are also scaled to best fit the data. The predicted TAE sensitively depends on the amplitude function, as shown in Fig. 8*B*, where we show TAE predicted from the amplitude lines shown in Fig. 8*A* (red, black, blue lines are results from the amplitude lines with corresponding colors in Fig. 8*A*; solid lines are from the model with the repulsive shifts of the preferred orientations and the dotted lines are from the model without). However, the overall shape of predicted TAE is closer to the actual TAE with the repulsive shifts. The TAE predicted without the repulsive shifts in general predict more TAE when the difference between the testing and adapting orientations is large. Because of the sensitivity of the predicted TAE on the amplitude function, we systematically vary the slope of the fitted line within -4 to 4 SE of the slope of the least-square-fit line (the red line in Fig. 8*A*), while also scaling the lines to best fit the data. For each fitted line, we compute, with the maximum-likelihood readout method, the predicted TAE, and calculate the mean square root difference between the predicted and observed TAE. The results are shown in Fig. 8*C* (with the repulsive shifts, sold line; without, dotted line). The difference achieves minimum within ± 2 SE of the slope both when the repulsive shifts of preferred orientations are included (solid cyan lines) and when not (dotted cyan lines). However, the minimum value of the difference is smaller with the repulsive shifts than that without. This can also be seen in Fig. 8*D*, where we plot the TAE best predicted from the model with the repulsive shifts (solid line) and that from the model without (dotted line). These results demonstrate that, within the scatter of the amplitude suppression data, the model with the repulsive shifts produces better prediction of the TAE.

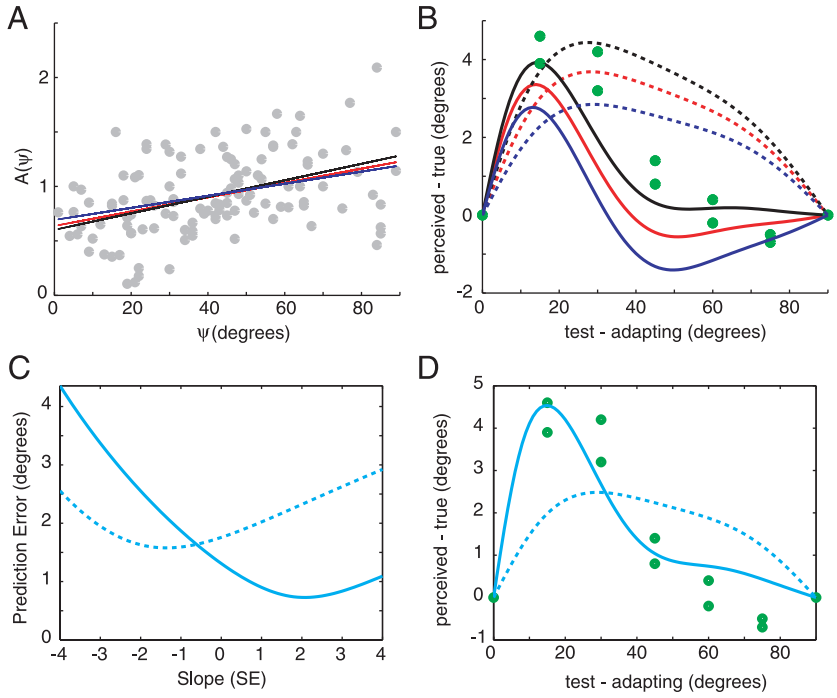

FIG. 8. Prediction errors of TAE with the adaptation-induced amplitude changes of tuning curves fitted with straight lines. *A*: scatterplot of the adaptation-induced change of amplitude $A(\psi)$ of neuron with label ψ (gray dots). These data are presented in Fig. 5 (green circles) by averaging over intervals of 15 deg. Three straight lines are shown. Red line is the least-square fit to the data (form $a + b\psi$, where $a = 0.63$, $b = 0.0066$); black is with the slope increased by a SE of the slope (0.0015) calculated in the least-square fit, and the overall scale adjusted to best fit the data; blue is the same as the black, but with the slope decreased by a SE. *B*: predicted TAE with (solid lines) and without (dotted lines) the repulsive shifts, compared with the actual TAE (green dots). Red, black, and blue lines are calculated with amplitude lines of corresponding colors shown in *A*. Overall angular dependency of the predicted TAE compares better to the actual TAE with the repulsive shifts than without. *C:* comparison of the prediction errors of TAE with (solid cyan line) and without (dotted cyan line) the repulsive shifts of the preferred orientations. Calculation of the TAE is the same as in Fig. 7, except that $A(\psi)$ is fitted with straight lines. Slope of the fitting line is systematically varied by −4 to 4 SE. Overall scale of the line is adjusted to best fit the amplitude data. For each line, TAE is calculated with and without repulsive shifts of the preferred orientations, and the prediction error is computed as the mean square root difference from the actual TAE data (green circles). Maximum-likelihood method is used as the readout method of perceived orientation. Minimum prediction error achieved is smaller with repulsive shifts than without. *D*: TAE best predicted in *C*. Result from the model with repulsive shifts of the preferred orientations (solid cyan line) fits better to the data (green dots) that that from the model without (dotted cyan line).

DISCUSSION

Our results demonstrate that the observed magnitude of the TAE is consistent with the amount of suppression and preferred orientation shift observed in V1 neurons. These two types of tuning curve changes have antagonistic effects on the TAE. The functional significance of this antagonism is unclear. One possibility is that relative suppression is an inevitable "design constraint" on neural circuitry and that the shift in preferred orientations has evolved to counter its effects. It is unlikely that our conclusion depends on the exact details of how the rest of the brain reads out the orientation information from the population responses of V1 neurons. This is evident from the agreement among the results using three different readout methods.

Past models of the TAE have relied only on the relative suppression of neural responses (Clifford et al. 2000; Coltheart 1971; Dong 1996; Sutherland 1961; Wainwright 1999). Our calculations indicate that these models are incomplete because they cannot reconcile quantitatively the amount of relative suppression with the magnitude of the TAE. To produce the observed magnitude of the perception shift, these models need less suppression than observed experimentally (Fig. 6, *right*); on the other hand, with the observed amount of suppression, the model predicts too much perceptual shift. Our model includes not only the suppression but also the repulsive shift of the preferred orientations and indicates that these two changes of the tuning curves together lead to a quantitatively consistent model of the TAE. Such consistency suggests that the psychophysical phenomenon of TAE can be explained by the properties of V1 neurons.

In this paper we have focused on the effects of prolonged adaptation (on the order of minutes). Recent physiological experiments have studied the effects of brief adaptation (<1 s) (Chung et al. 2002; Dragoi et al. 2002; Felsen et al. 2002; Muller et al. 1999). These experiments demonstrate that a brief adaptation can also cause the tuning curves to suppress relatively and shift repulsively, similar to that during prolonged adaptation. However, the TAE is weak, if any, for brief adaptation (Magnussen and Johnsen 1986). A possibility is that in this case the repulsive shift cancels the shift of perception that can arise from the relative suppression, resulting in a weak TAE. This hypothesis can be quantitatively tested in the same way as in this paper by comparing the observed amount of suppression to that calculated with the observed shifts of the preferred orientations alone.

Previously, while simulating the tilt illusion, a psychophysical phenomenon related to the TAE, Gilbert and Wiesel (1990) observed the opposing effects of amplitude suppres-

sion and repulsive shifts of preferred orientations on orientation perception. Our mathematical analysis goes beyond this qualitative observation and unveils a quantitative relationship between the suppression and the shifts of perception and preferred orientations. Such relationships enable us to check the consistency between psychophysical and physiological data. The relationship is also useful as a caution against an oversimplified conclusion that the directions of shifts in the tuning curves and the perceived orientations are always opposite (Teich and Qian 2003; Yao and Dan 2001). As our analysis shows, the relative directions depend on the change of the amplitudes of the tuning curves. Inferring perception from tuning curves must be done through a careful analysis of the firing rate function constructed from the tuning curves.

We briefly note some general constraints on the source of the suppression. Suppression in V1 neurons could arise from changes within the cortex itself or from changes in the inputs to the cortex. The latter type of change, although no doubt present, does not seem to be important for the psychological and physiological experiments considered in this paper. Adaptation is induced with a drifting grating, which tends to activate all LGN neurons equally over time because they are at most weakly tuned to orientation (Hubel and Wiesel 1961). Therefore, any adaptation of thalamocortical input is expected to be unspecific for orientation. Thus, the locus of orientation-specific adaptation is likely to be the cortex (Carandini and Heeger 1994; Movshon and Lennie 1979). One plausible scenario involves adaptation of the excitatory connections between neurons tuned to the adapting orientation, which would cause the responses of these neurons to be suppressed (Dong 1996; Felsen et al. 2002; Teich and Qian 2003). Quantitative support in favor of this idea comes from independent studies of the effects of recurrent excitation. Recurrent excitation is estimated to amplify cortical responses by a factor of about two or three (Ferster et al. 1996). Therefore, weakening of recurrent excitation by adaptation would be expected to reduce the amplitudes of tuning curves by up to this factor, which is in rough quantitative accord with the tuning-curve suppression depicted in Fig. 6. Another possible source of adaptation within the cortex is reduction in spiking of neurons attributed to activation of long-lasting hyperpolarizing currents after prolonged spiking activity (Carandini and Ferster 1997; Sanchez-Vives et al. 2000).

We have shown that the TAE is consistent with the physiological data obtained from anesthetized cat V1 neurons. Two caveats should be noted. First, the psychophysics of the TAE is based on human experiments. However, the function and organization of V1 is quite similar across mammalian species and V1 neurons likely behave similarly under adaptation. Indeed, several recent studies have demonstrated neural correlates of high-level perception in human V1 (Lee et al. 2005; Ress and Heeger 2003). It might also be possible to test the TAE and measure V1 neuron responses in the same animal. Quantitative consistency of the psychophysical and physiological data in such experiments should provide a stronger ground for concluding that the TAE arises from the properties of V1 neurons. Second, our model relies on a simple assumption: the unadapted tuning curves of neurons are the same and adaptation-induced changes of the tuning curves depends only on the distance between the labels of the neurons and the adapting orientation. This assumption, which is also the basis of most of the previous models of the TAE (Clifford et al. 2000; Coltheart 1971; Sutherland 1961; Wainwright 1999), enables us to derive in compact form the quantitative relationship between the changes of the tuning curves and the TAE. In reality, the tuning curves have a wide range of shapes and adaptation-induced changes of these curves also depend on the locations of neurons relative to the orientation map (Dragoi et al. 2001). Our model does not account for the observed diversity of neuron properties. It remains to be seen how inclusion of this diversity, which inevitably requires large-scale simulations of the visual cortex, might modify our results.

Besides the TAE, there are other adaptation-induced aftereffects such as the motion aftereffect (Huk et al. 2001) and the spatial frequency aftereffect (Humanski and Wilson 1993). Population coding models similar to the one in this paper can also be useful for quantitatively checking the consistency between psychophysical and physiological data in these aftereffects. A recent study of motion adaptation in MT neurons in anesthetized monkeys demonstrates an attractive shift in the direction tuning of these neurons, toward the adapting direction (Kohn and Movshon 2003, 2004). Whether such an attractive shift in direction tuning generalizes to other kinds of adaptation, such as orientation adaptation, in visual cortical areas remains to be examined. However, these findings raise the issue of the perceptual locus of adaptation-induced changes, in particular whether specific visual areas are privileged sites for specific percepts and whether there are different mechanisms and consequences of pattern adaptation in different cortical areas. A more complete description of neuronal responses and the consequences of pattern adaptation in different areas of visual cortex will be required to resolve these issues.

APPENDIX

In the following we describe the procedures for calculating $A(\psi)$ with the winner-take-all method. For convenience, we let the adapting orientation be at 0, and discuss only the case of $\psi > 0$ (the case for $\psi < 0$ is similar). The overall scaling of $A(\psi)$ is not determined from the calculations. Here we simply set $A(0) = 1$.

In the winner-take-all method, the label of the neuron that fires the most in the population equals the perceived orientation. The population response curve to a stimulus ϕ is given by $F(\psi, \phi)$ with ϕ held constant. The peak location of this curve is given by setting to zero the partial derivative of the rate function with respect to the neuron label, that is

$$0 = \frac{\partial F(\psi, \phi)}{\partial \psi} = \frac{dA(\psi)}{d\psi} \exp\left\{ -\frac{[\phi - \phi_n(\psi)]^2}{2\sigma(\psi)^2} \right\} + A(\psi) \exp\left\{ -\frac{[\phi - \phi_n(\psi)]^2}{2\sigma(\psi)^2} \right\} \times \left\{ \frac{[\phi - \phi_n(\psi)]}{\sigma(\psi)^2} \frac{d\phi_n(\psi)}{d\psi} + \frac{[\phi - \phi_n(\psi)]^2}{\sigma(\psi)^3} \frac{d\sigma(\psi)}{d\psi} \right\} \quad (A1)$$

Here we used *Eq. 1* for the rate function $F(\psi, \phi)$. Rearranging terms in above equation, we find

$$\frac{dA(\psi)}{d\psi} = A(\psi) \frac{\phi_n(\psi) - \phi}{\sigma(\psi)^2} \left[\frac{d\phi_n(\psi)}{d\psi} - \frac{\phi_n(\psi) - \phi}{\sigma(\psi)} \frac{d\sigma(\psi)}{d\psi} \right] \quad (A2)$$

Solving the above equation for ψ, we obtain the perceived orientation of stimulus ϕ. In other words, the solution of the above equation is given by $\psi = \psi_p(\phi)$. An equivalent expression of the solution is $\phi = \psi_p^{-1}(\psi)$, where ψ_p^{-1} is the inverse function of the perception line $\psi_p(\phi)$. Therefore, the above equation can also be written as

$$\frac{dA(\psi)}{d\psi} = A(\psi)\frac{\phi_n(\psi) - \psi_p^{-1}(\psi)}{\sigma(\psi)^2}\left[\frac{d\phi_n(\psi)}{d\psi} - \frac{\phi_n(\psi) - \psi_p^{-1}(\psi)}{\sigma(\psi)}\frac{d\sigma(\psi)}{d\psi}\right] \quad (A3)$$

This equation gives the relationship among the amplitude function $A(\psi)$, the perception line $\psi_p(\phi)$, the neuron line $\phi_n(\psi)$, and the width parameter $\sigma(\psi)$. Notice that the changes of the amplitudes of the tuning curves, depicted by the derivative on the left-hand side of the above equation, cannot be arbitrary. Noting that

$$\frac{1}{A(\psi)}\frac{dA(\psi)}{d\psi} = \frac{d \ln A(\psi)}{d\psi}$$

we solve the above differential equation to find

$$A(\psi) = \exp\left\langle \int_0^{\psi} d\psi' \frac{[\phi_n(\psi') - \psi_p^{-1}(\psi')]}{\sigma(\psi')^2}\left\{\frac{d\phi_n(\psi')}{d\psi'} - \frac{[\phi_n(\psi') - \psi_p^{-1}(\psi')]}{\sigma(\psi')}\frac{d\sigma(\psi')}{d\psi'}\right\}\right\rangle \quad (A4)$$

Numerically integrating the above equation gives the amplitude function $A(\psi)$ with given neuron and perception lines, as well as the tuning width parameters.

For the adapted state, we can explicitly evaluate *Eq. A4* with piecewise-linear approximations to the neuron and the perception lines and assuming that the tuning width parameter is a constant σ. The neuron line is approximated with two straight lines determined by three pairs of neuron label and the preferred orientation: (0, 0), (Ψ, $\Psi + \Delta$), (90, 90), where Ψ is the label of the neuron that shows the maximum preferred orientation shift Δ. This gives the following expression for the approximated neuron line

$$\phi_n(\psi) = \begin{cases} k_1\psi & \text{for } 0 < \psi < \Psi \\ 90 + k_2(90 - \psi) & \text{for } \Psi < \psi < 90 \end{cases} \quad (A5)$$

Here

$$k_1 = \frac{\Psi + \Delta}{\Psi} \text{ and } k_2 = \frac{\Psi + \Delta - 90}{\Psi - 90}$$

are the slopes of the two lines. Similarly, the perception line is approximated with two straight lines determined by three pairs of the stimulus orientation and the perceived orientation: (0, 0), (Φ, $\Phi + \Delta$), (90, 90), where Φ is the orientation of the stimulus that shows the maximum perception shift δ. The inverse function of the approximated perception lines is given by the following equation

$$\psi_p^{-1}(\psi) = \begin{cases} k_3\psi & \text{for } 0 < \psi < \Phi + \delta \\ 90 + k_4(90 - \psi) & \text{for } \Phi + \delta < \psi < 90 \end{cases} \quad (A6)$$

Here

$$k_3 = \frac{\Phi}{\Phi + \delta} \text{ and } k_4 = \frac{\Phi - 90}{\Phi + \delta - 90}$$

are the slopes of the two lines of the inverse function. Plugging in *Eqs. A5* and *A6* into *Eq. A4* yields the following expression for the amplitude modulation:

Case 1: $\Psi \leq \Phi + \delta$.

In this case, we have

$$A(\psi) = \begin{cases} \exp\left(\frac{a\psi^2}{2\sigma^2}\right) & \text{for } 0 < \psi < \Psi \\ \exp\left(\frac{b\psi^2 + c\psi + d}{2\sigma^2}\right) & \text{for } \Psi \leq \psi < \Phi + \delta \\ \exp\left(\frac{f\psi^2 + g\psi + h}{2\sigma^2}\right) & \text{for } \Phi + \delta < \psi \leq 90 \end{cases} \quad (A7)$$

Here the constants are given by $a = k_1(k_1 - k_3)$, $b = k_2(k_2 - k_3)$, $c = 180k_2(1 - k_2)$, $d = 90^2(1 - k_2)^2 + k_3(k_2 - k_1)\Psi^2$, $f = k_2(k_2 - k_4)$, $g = 180k_2(k_4 - k_2)$, and $h = k_3(k_2 - k_1)\Psi^2 + k_2(k_4 - k_3)(\Phi + \delta)^2 + 90^2(1 - k_2)^2 + 180k_2(1 - k_4)(\Phi + \delta)$.

Case 2: $\Phi + \delta < \Psi$.

In this case, we have

$$A(\psi) = \begin{cases} \exp\left(\frac{a\psi^2}{2\sigma^2}\right) & \text{for } 0 < \psi < \Phi + \delta \\ \exp\left(\frac{u\psi^2 + v\psi + w}{2\sigma^2}\right) & \text{for } \Phi + \delta \leq \psi < \Psi \\ \exp\left(\frac{f\psi^2 + g\psi + s}{2\sigma^2}\right) & \text{for } \Psi < \psi \leq 90 \end{cases} \quad (A8)$$

Here the constants are given by $u = k_1(k_1 - k_4)$, $v = -180k_1(1 - k_4)$, $w = k_1(k_4 - k_3)(\Phi + \delta)^2 + 180k_1(1 - k_4)(\Phi + \delta)$, and $s = k_1(k_4 - k_3)(\Phi + \delta)^2 + k_4(k_2 - k_1)\Psi^2 + 90^2(1 - k_2)^2 + 180(1 - k_4)(k_1(\Phi + \delta) + (k_2 - k_1)\Psi)$.

As can be seen from *Eqs. A7* and *A8*, piecewise-linear approximations of the neuron and the perception lines result in a piecewise-Gaussian surface for the rate function. Away from the adapting orientation at 0, the amplitude function increases exponentially with the square of the distance of the neuron label from the adapting orientation. The rate factor of this exponential can be expressed as follows when the shifts of the perceptions and preferred orientations are small compared to Φ and Ψ, respectively

$$\frac{a}{2\sigma^2} \approx \frac{1}{2\sigma^2}\left(\frac{\Delta}{\Psi} + \frac{\delta}{\Phi}\right) \quad (A9)$$

The above equation shows that larger repulsive shifts of perception and repulsive shifts of the preferred orientation add up to cause a faster rise of the amplitudes of the tuning curves away from the adapting orientation.

GRANTS

D. Z. Jin was supported by the Huck Institute of Life Sciences at The Pennsylvania State University, H. S. Seung was supported by Howard Hughes Medical Institute, V. Dragoi was supported by the McDonnell–Pew Foundation, and M. Sur received support from the National Institutes of Health.

REFERENCES

Carandini M and Ferster D. A tonic hyperpolarization underlying contrast adaptation in cat visual cortex. *Science* 276: 949–952, 1997.

Carandini M and Heeger DJ. Summation and division by neurons in primate visual cortex. *Science* 264: 1333–1336, 1994.

Chung S, Li X, and Nelson SB. Short-term depression at thalamocortical synapses contributes to rapid adaptation of cortical sensory responses in vivo. *Neuron* 34: 437–446, 2002.

Clifford CW, Pearson J, Forte JD, and Spehar B. Colour and luminance selectivity of spatial and temporal interactions in orientation perception. *Vision Res* 43: 2885–2893, 2003.

Clifford CW, Wenderoth P, and Spehar B. A functional angle on some after-effects in cortical vision. *Proc R Soc Lond B Biol Sci* 267: 1705–1710, 2000.

Coltheart M. Visual feature-analyzers and the aftereffects of tilt and curvature. *Psychol Rev* 78: 114–121, 1971.

Dong DW. *Associative Decorrelation Dynamics in Visual Cortex,* edited by Sirosh J, Miikkulainen R, and Choe Y. Austin, TX: UTCS Neural Networks Research Group (www.cs.utexas.edu/users/nn/web-pubs/htmlbook96/dong), 1996.

Dragoi V, Rivadulla C, and Sur M. Foci of orientation plasticity in visual cortex. *Nature* 411: 80–86, 2001.

Dragoi V, Sharma J, Miller EK, and Sur M. Dynamics of neuronal sensitivity in visual cortex and local feature discrimination. *Nat Neurosci* 5: 883–891, 2002.

Dragoi V, Sharma J, and Sur M. Adaptation-induced plasticity of orientation tuning in adult visual cortex. *Neuron* 28: 287–298, 2000.

Felsen G, Shen YS, Yao H, Spor G, Li C, and Dan Y. Dynamic modification of cortical orientation tuning mediated by recurrent connections. *Neuron* 36: 945–954, 2002.

Ferster D, Chung S, and Wheat H. Orientation selectivity of thalamic input to simple cells of cat visual cortex. *Nature* 380: 249–252, 1996.

Georgopoulos AP, Kalaska JF, Caminiti R, and Massey JT. On the relations between the direction of two-dimensional arm movements and cell discharge in primate motor cortex. *J Neurosci* 2: 1527–1537, 1982.

Gibson JJ and Radner M. Adaptation, aftereffect and contrast in the perception of tilted lines: I. Quantitative studies. *J Exp Psychol* 20: 453–467, 1937.

Gilbert CD and Wiesel TN. The influence of contextual stimuli on the orientation selectivity of cells in primary visual cortex of the cat. *Vision Res* 30: 1689–1701, 1990.

He S and MacLeod DI. Orientation-selective adaptation and tilt after-effect from invisible patterns. *Nature* 411: 473–476, 2001.

Hubel DH and Wiesel TN. Integrative action in the cat's lateral geniculate body. *J Physiol* 155: 385–398, 1961.

Hubel DH and Wiesel TN. Receptive fields, binocular interaction and functional architecture in the cat's visual cortex. *J Physiol* 160: 106–154, 1962.

Huk AC, Ress D, and Heeger DJ. Neuronal basis of the motion aftereffect reconsidered. *Neuron* 32: 161–172, 2001.

Humanski RA and Wilson HR. Spatial-frequency adaptation: evidence for a multiple-channel model of short-wavelength-sensitive-cone spatial vision. *Vision Res* 33: 665–675, 1993.

Kohn A and Movshon JA. Neuronal adaptation to visual motion in area MT of the macaque. *Neuron* 39: 681–691, 2003.

Kohn A and Movshon JA. Adaptation changes the direction tuning of macaque MT neurons. *Nat Neurosci* 7: 764–772, 2004.

Lee SH, Blake R, and Heeger DJ. Traveling waves of activity in primary visual cortex during binocular rivalry. *Nat Neurosci* 8: 22–23, 2005.

Magnussen S and Johnsen T. Temporal aspects of spatial adaptation. A study of the tilt aftereffect. *Vision Res* 26: 661–672, 1986.

Mitchell DE and Muir DW. Does the tilt after-effect occur in the oblique meridian? *Vision Res* 16: 609–613, 1976.

Movshon JA and Lennie P. Pattern-selective adaptation in visual cortical neurones. *Nature* 278: 850–852, 1979.

Muller JR, Metha AB, Krauskopf J, and Lennie P. Rapid adaptation in visual cortex to the structure of images. *Science* 285: 1405–1408, 1999.

Paradiso MA. A theory for the use of visual orientation information which exploits the columnar structure of striate cortex. *Biol Cybern* 58: 35–49, 1988.

Pouget A, Dayan P, and Zemel R. Information processing with population codes. *Nat Rev Neurosci* 1: 125–132, 2000.

Press WH, Flannery BP, Teukolsky SA, and Vetterling WT. *Numerical Recipes in C.* Cambridge, UK: Cambridge Univ. Press, 1988.

Ress D and Heeger DJ. Neuronal correlates of perception in early visual cortex. *Nat Neurosci* 6: 414–420, 2003.

Sanchez-Vives MV, Nowak LG, and McCormick DA. Cellular mechanisms of long-lasting adaptation in visual cortical neurons in vitro. *J Neurosci* 20: 4286–4299, 2000.

Sutherland NS. Figural after-effects and apparent size. *Q J Exp Psychol* 13: 222–228, 1961.

Swindale NV. Orientation tuning curves: empirical description and estimation of parameters. *Biol Cybern* 78: 45–56, 1998.

Teich AF and Qian N. Learning and adaptation in a recurrent model of V1 orientation selectivity. *J Neurophysiol* 89: 2086–2100, 2003.

Vogels R. Population coding of stimulus orientation by striate cortical cells. *Biol Cybern* 64: 25–31, 1990.

Wainwright MJ. Visual adaptation as optimal information transmission. *Vision Res* 39: 3960–3974, 1999.

Watkins DW and Berkley MA. The orientation selectivity of single neurons in cat striate cortex. *Exp Brain Res* 19: 433–446, 1974.

Yao H and Dan Y. Stimulus timing-dependent plasticity in cortical processing of orientation. *Neuron* 32: 315–323, 2001.